A single chemosensor for multiple analytes: fluorogenic and ratiometric absorbance detection of Zn^{2+}, Mg^{2+} and F^-, and its cell imaging

LI Li[a], SHEN Yun[a], ZHAO Yuan-Hui[a], MU Lan[a], ZENG Xi*[,a], Carl Redshaw[b] WEI Gang*[,c]

[a] Key Laboratory of Macrocyclic and Supramolecular Chemistry of Guizhou Province; School of Chemistry and Chemical engineering, Guizhou University, Guiyang 550025, China

[b] Department of Chemistry, University of Hull, Hull HU6 7RX, U.K.

[c] CSIRO Manufacturing Flagship, PO Box 218, NSW 2070, Australia

Abstract: A simple coumarin based sensor **1** has been synthesized from the condensation reaction of 7-hydroxycoumarin and ethylenediamine via the intermediate 7-hydroxy-8-aldehyde-coumarin. As a multiple analysis sensor, **1** can monitor Zn^{2+} with the fluorescence enhanced at 457 nm, meanwhile formed absorption ratio at 290 nm, 350 nm and 420 nm in DMF/H_2O (1/4, v/v) medium. Sensor **1** can also monitor Mg^{2+} with the fluorescence enhanced at 430 nm, meanwhile formed absorption ratio at 290 nm, 370 nm and 430 nm in DMF medium through the interaction of chelation enhance fluorescence (CHEF) with metal ions. Furthermore, **1** also can monitor F^- with the fluorescence enhanced at 460 nm, and formed absorption ratio at 290 nm and 390 nm in DMF medium simultaneously via hydrogen bonding and deprotonation with F^- anion. Spectral titration, isothermal titration calorimetry and mass spectrometry revealed that the sensor formed a 1:1 complex with Mg^{2+}, Zn^{2+} or F^-, with stability constants of 4.5×10^6, 3.4×10^6, 8.0×10^4 M^{-1} respectively. The complexation of the ions by **1** was an exothermic reaction driven by entropy processes. Furthermore, the sensor exhibits good membrane-permeability and was capable of monitoring at the intracellular Zn^{2+} level in living cells.

Keywords: Coumarin sensor; Fluorogenic and ratiometric absorbance; Multiple analysis; Zn^{2+}/Mg^{2+}/F^-; Cell imaging

Introduction

Metals are indispensable for life, as they are involved in many fundamental biological processes, including osmotic regulation, catalysis, metabolism, biomineralization, and signaling [1]. Amongst the biologically important metal ions, the Zn^{2+} and Mg^{2+} ions are known for their ability in widespread applications. Zinc is the second most abundant transition metal in the human body, and it plays a critical role in enzyme regulation structure and function, neural signal transmission, and gene expression [2-5]. The magnesium ion is one of the most abundant divalent cations in cells and can play vital roles in enzyme-driven biochemical reactions, proliferation of cells, and stabilization of DNA conformation [6-8]. Numerous small anions, which play vital roles in human life, exist within organisms and in the external environment [9]. Detection and quantification of metal ions and anion found in biological systems and in the environment remains an active area of research, as these ions can be either quite beneficial or toxic to human health [10, 11]. Therefore, the assessment and understanding of metal ions and anions and their distribution in living systems could be crucial to obtaining insight into metal homeostasis, as well as into related diseases [12].

Fluorescent sensors have been developed as a useful tool to sense *in vitro* and *in vivo* biologically important ions because of their specific and sensitive monitoring with fast response time [13, 14]. A large number of fluorescent sensors for Zn^{2+} have been reported, exhibiting high selectivity and sensitivity over other biologically essential metal ions in specific ranges of concentration [16-18]. Mg^{2+} is one of the most abundant divalent cations in cells and is closely connected with many cellular and pathological processes [6, 19]. Until now, there are few reports relating to fluorescent sensors for the determination of Mg^{2+} [20-23].

As the smallest anion, F^- has unique chemical properties; its recognition and detection have received considerable attention because it is very important to measure the concentration of F^- for human health and environment protection [24, 25]. In fact, numerous fluorescent and chromogenic sensors have been reported to selectively detect F^-, which contain receptors based on Lewis-acidic boron as well as sensors utilizing hydrogen bonding [26-28].

Recently, single sensor for multiple analytes have become very popular among analysts, due to their good sensing performance, clear signaling mechanism, fast detection time and relative cost. Finding new types of sensor possessing simple molecular structures for multifunction recognition is a significant area of research. Examples of such sensors are Zn^{2+}/F^- [29], $Zn^{2+}/Cd^{2+}/Co^{2+}$ [30], $Zn^{2+}/Al^{3+}/Fe^{3+}/Fe^{2+}$ [31], CN^-/F^- [32], Cu^{2+}/Hg^{2+} [33]. Our group has also recently reported a sensor for

Al^{3+}/F$^-$ [34].

Coumarins are well known fluorophores with high quantum yields, high photo-stability and a backbone which is readily modified. A number of excellent coumarin-based fluorescent sensors for Cu^{2+} [35], Zn^{2+} [36], Al^{3+} [37], pH [38], and thiols [39] have been reported, but most of them were employed in single target detection. Due to the close relationship between Zn^{2+}, Mg^{2+} or F$^-$ and human health and the environment, it is crucial to develop multi-function and multi-analysis sensors.

Herein, we present a simple coumarin-based sensor, which is synthesized by the condensation reaction from between 7-hydroxycoumarin and ethylenediamine, and which can conveniently and highly selectively measure Mg^{2+}, Zn^{2+} and F$^-$ in different solution media by fluorescence enhancement, and ratiometrically absorbance, it can serve as one sensor for multiple analytes, and is suitable for the preferential sensing of Mg^{2+}, Zn^{2+} and F$^-$ in the presence of other biologically relevant ions and is suitable for the monitoring of Zn^{2+} ions in living cells.

2. Experimental

2.1. Materials and equipments

7-Hydroxycoumarin, ethanediamine, TFA (trifluoroacetic acid), dichloromethane, pyridine, hexamethylene tetramine were purchased commercially (Aldrich and Alfa Aesar Chemical Co., Ltd.). The solutions of the metal ions were prepared from their nitrate salts. All the anions used were as tetra-*n*-butylammonium salts (Sigma-Aldrich Chemical Co.), and were stored in a desiccator under vacuum containing self-indicating silica, and were then used without any further purification. Other chemicals used in this work were of analytical grade and were used without further purification. Double distilled water was used throughout.

All fluorescence measurements were made on a Cary Eclipse Fluorescence Spectrometer (Varian) in a 1 cm quartz cell. UV-Vis absorption spectra were recorded on a UV-1800 spectrophotometer (Beijing General Instrument Co., China) in a 1 cm quartz cell. ^{1}H NMR spectra were measured on a Nova-400 NMR spectrometer (Varian) and WNMR-I 500 MHz NMR (at the Wuhan Institute of Physics and Mathematics, Chinese Academy of Sciences) spectrometer at room temperature using TMS as an internal standard. ESI-MS spectra were recorded on a HPLC-MSD-Trap-VL spectrometer (Agilent). IR spectra were obtained using a Vertex 70 FT-IR spectrometer (Bruker). Isothermal titration calorimetry (ITC) experiments were performed using an isothermal titration

calorimeter a Nano ITC (TA); Fluorescence imaging was conducted on a Ti (Nikon) fluorescent inverted phase contrast microscope.

2.2. Solution preparation

A stock solution of 0.1 mM sensor **1** was obtained by dissolving the requisite amount of **1** in DMF solvent. A standard stock solution of 10 mM Zn^{2+} (Mg^{2+}) was prepared by dissolving an appropriate amount of zinc nitrate (magnesium nitrate) in water and adjusting the volume to 100 mL in a volumetric flask.

A standard stock solution of 10 mM F^- was prepared by dissolving an appropriate amount of tetrabutylammonium salt in DMF and adjusting the volume to 100 mL in a volumetric flask.

The salts used in other stock solutions of metal ions were nitrate salts, and the anions were tetrabutylammonium salts.

All the measurements were made according to the following procedure. To 10 mL volumetric flask containing different amounts of metal ion or anion, requisite amounts of the solution of sensor **1** was added directly with micropipette, for Zn^{2+}, then diluted with DMF/H_2O (1/4, v/v) mixed solvent to 10 mL, for Mg^{2+}, diluted with DMF/H_2O (49/1, v/v) to 10 mL, for F^-, diluted with DMF to 10 mL. Fluorescence and UV-vis spectra were measured after addition of the ions at room temperature to equilibrium. Fluorescence measurements were carried out with excitation and mission slit width of 10 and 10 nm.

The ITC experiment consisted of 25 consecutive injections (10 μL) of ion in DMF solution (Mg^{2+}, F^-, 0.1 mM) into the microcalorimetric reaction cell (1mL) charged with a DMF solution of sensor **1** (10 μM) at 288.15 K. The heat of reaction was corrected for the heat of dilution of the ion solution determined in the separate experiments. All solutions were degassed prior to titration experiment by sonication. Computer simulations (curve fitting) were performed using the Nano ITC ananlyze software.

Cell culture and fluorescence imaging

The PC3 cells were grown in Roswell Park Memorial Institute-1640 supplemented with 10 % fetal bovine serum, 100 U/mL penicillin and 100 μg/mL streptomycin at 37 ℃ and 5% CO_2. One day before imaging, the cells were seeded in 6-well flat-bottomed plates. The next day, the PC3 cells were incubated with 10 μM **1** for 30 min at 37 ℃ in humidified environment of 5% CO_2 and then washed with fresh culture medium three times to remove the remaining **1**. Before incubating with 50 μM Zn^{2+} for another 30 min, cells were rinsed with fresh culture medium three times again,

then the fluorescence imaging of intracellular Zn^{2+} was observed under inverted fluorescence microscope excited with UV lamp. The PC3 cells only incubated with 10 μM **1** for 30 min at 37 ℃ and 5% CO_2 were as a blank control.

2.3. Synthesis of sensors

The intermediate was synthesized from 7-hydroxycoumarin and acetic anhydride in dichloromethane solvent, then using trifluoroacetic acid (TFA) as catalyst, reaction with hexamethylenetetramine was conducted to afford 7-hydroxy-8-aldehyde coumarin, and then further condensation to give sensor **1**. The synthetic route was carried out as outlined in Scheme 1:
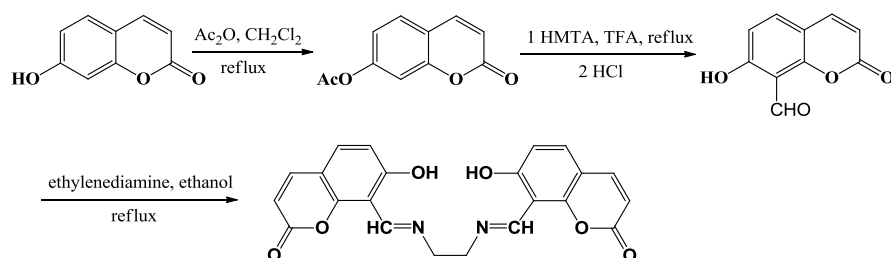
Scheme 1 Synthesis of the sensor **1**.

Synthesis of 7- acetic anhydride coumarin

To a solution of 7-hydroxycoumarin (9.3g, 57.3 mM) in dichlorormethane (120 mL) was added acetic anhydride (11.7g, 114.6 mM) and pyridine (7-8 drops). The mixture was heated under reflux for 12 h. Following removal of the solvent by evaporation, water (80 mL) was added to the mixture, which was extracted with ethyl acetate (120 mL×3), the organic layer was washed with distilled water (30 mL×2), and then was washed with saturated salt water 30 mL, and the organic layer was dried with anhydrous sodium sulfate overnight. The organic layer was separated and the solvents were evaporated. The crude product was purified by column chromatography over silica gel using chloroform as the eluent to afford the white solid, 11.78 g, 95.4 ％.

Synthesis of 8- formyl-7-hydroxy-coumarin

In an ice bath, to a solution of 7-hydroxycoumarin (15g, 73.51 mM) in trifluoroacetic acid (TFA, 100 mL) was added hexamethylenetetramine (15g, 106.26 mM). The mixture was reacted at 0 ℃ for 1 h, and then the temperature was gradually raised to room temperature，and then heated under reflux for 8 h. Following removal of the solvent by evaporation, water (150 mL) was added to the mixture，and the mixture was heated under 60 ℃ for 0.5 h. Following filtration, the residue was extracted with chloroform (150 mL×3), the organic layer was washed with distilled water (20

mL×2), and then was washed with saturated salt water 20 mL, and the organic layer was dried with anhydrous sodium sulfate overnight. The organic layer was separated and the solvents were evaporated. The crude product was purified by column chromatography over silica gel using chloroform/ methanol (100/1, v/v) as the eluent to afford the milky solid, 2.61 g, 18.6 %.

Synthesis of sensor **1**

To a solution of 8-formyl-7-hydroxy-coumarin (600 mg, 3.16 mM) in dry ethanol (70 mL) was added dropwise ethanediamine (90mg, 1.58 mM）which had dissolved in ethanol (30 mL). The mixture was filtered and was recrystallization from chloroform and methanol to afford a pale yellow solid, 510 mg, 80.5 %. m.p. 300 ℃; ^{1}H NMR (DMSO-d_6, 400M Hz), δ (ppm): 4.06 (s, 2H), 6.10 (d, 1H, J= 9.6 Hz), 6.55 (d, 1H, J=9.2 Hz), 7.52 (d, 1H, J= 8.8 Hz), 7.86 (d, 1H, J= 9.2 Hz), 8.93 (s, 1H), 14.39 (s, 1H); M/z (ESI): 427.0 ([M+Na]$^+$), calcd for $C_{22}H_{16}N_2O_6$= 404.37. IR (KBr, cm^{-1}) ν: 3445, 2921, 1731, 1722, 1635, 1596, 1236, 1113, 784. (Figs. S1~S3)

3. Results and discussion

3.1 Spectra studies

3.1.1 Absorption spectra characteristics for ions

In DMF/H$_2$O (1/4, v/v) mixed solvent, the absorption spectrum of **1** showed three absorption bands at 290 nm, 355 nm and 420 nm. Upon addition of Zn^{2+}, the absorbance peaks at around 290 nm and 420 nm of **1** significantly diminished, meanwhile the absorption band at around 350 nm red-shifted and significantly increased (Fig. 1A). By contrast, the addition of 20 eq. of various other metal ions, namely Mg^{2+}, Li$^+$, Na$^+$, K$^+$, Ca^{2+}, Hg^{2+}, Ba^{2+}, Pb^{2+}, Cd^{2+}, Co^{2+}, Ni^{2+}, Sr^{2+}, Cr^{3+}, Cu^{2+}, Ag$^+$, Al^{3+} or Fe^{3+}, resulted in only negligible changes to the absorption spectrum of **1**. Such results indicated that **1** has a good selectivity for Zn^{2+}. Upon titration of **1** (10 μM) with Zn^{2+} (0 ~ 20 μM), the absorption bands at 290 nm, 420 nm gradually decreased in intensity, whereas the absorption band at 347 nm increased and shifted to 355 nm with a shoulder at 370 nm, generating two isosbestic points at 330 nm and 400 nm, which indicated the formation of a new complex between **1** and Zn^{2+} (Fig. 1B), present having a certain stoichiometric ratio between the **1** and Zn^{2+} (Fig. 1B inset). The formation of the new band at 355 nm is attributed to the interaction of Zn^{2+} ions with the imino nitrogen atoms and hydroxyl oxygen atoms leading to intramolecular charge transfer (ICT) from the comarine moiety to the imino group. The absorbance ratio (A$_{355}$/A$_{420}$) showed a clear

sigmoid dependence on the Zn^{2+} concentration, and it is noteworthy that the ratiometric absorbance change could be potentially useful for the quantitative determination of Zn^{2+}.
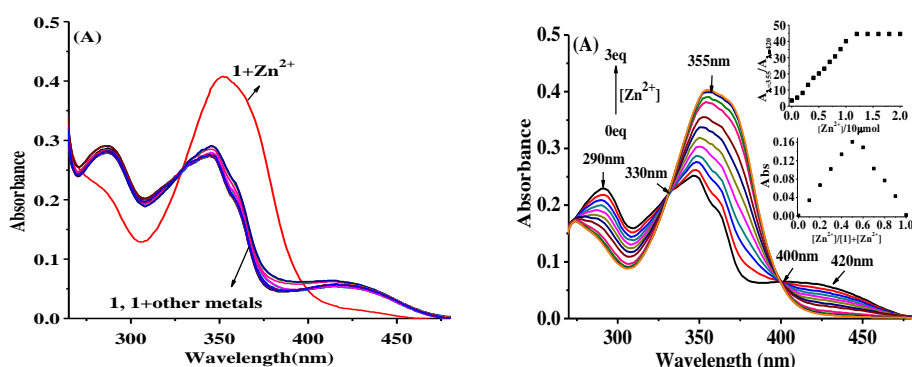
Fig. 1 (A) Absorption spectrum of **1** (10 μM) upon the addition of 20 eq. metal ions in DMF/H$_2$O (1/4, v/v); (B) Absorbance spectrum for titration of **1** (10 μM) with Zn^{2+}. Inset shows variation of ratio absorbance against the number of equivalents of ions; data and Job's plot data. $A_{355\,nm}/A_{420\,nm}$

In contrast, in a DMF/H$_2$O (49/1, v/v) mixed solvent system, **1** (10 μM) exhibited ratiometric behaviour with Mg^{2+} (Fig. 2A), whilst other tested metal ions including Zn^{2+} resulted in negligible changes to the absorption spectrum of **1**, indicated that **1** has a good selectivity for Mg^{2+} in DMF/H$_2$O (49/1, v/v) medium. The addition of increasing amounts of Mg^{2+} ion (Fig. 2B) results in a decrease in the absorption at 290 nm and 430 nm and the formation of a new intense red shifted absorption band at 370 nm with a shoulder at 355nm, and well-defined isosbestic points at 335 nm and 405 nm. This further demonstrated that a stable complex was present having a certain stoichiometric ratio between the **1** and Mg^{2+} formed under these conditions (Fig. 2B inset). The absorbance ratio (A_{370}/A_{420}) showed a clear sigmoid dependence on the Mg^{2+} concentration, and it is noteworthy that the ratiometric absorbance change could be potentially useful for the quantitative determination of Mg^{2+}.
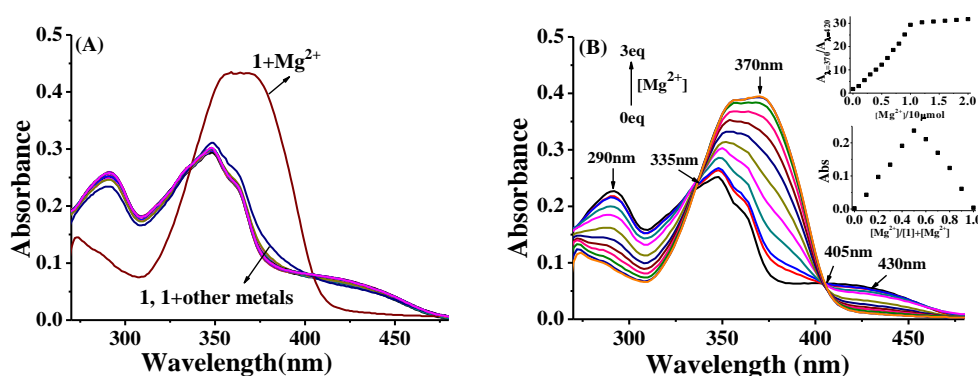
Fig. 2 (A) Absorption spectra of **1** (10 μM) upon the addition of 20 eq. metal ions in DMF/H$_2$O (49/1, v/v); (B)

Absorbance spectra titration of **1** (10 μM) with Mg^{2+}. Inset shows the variation of ratio absorbance against the number of equivalents of ions; data and Job's plot data. $A_{370\ nm}/A_{430\ nm}$

The fluorescence intensity of **1** (10 μM) in different volume fractions of water in a DMF/H_2O mixed solvent system were very low at 350 nm excitation wavelength, and was unaffected by the volume fraction of water. However, the fluorescence intensity of **1** was affected in the presence of 20 eq. of Zn^{2+} and Mg^{2+} (Fig 3A). For example, in DMF/H_2O (49/1, v/v) solvent, the intensity of **1** was significantly enhanced at 430 nm on addition of Mg^{2+}, whereas there was only a slight increase of intensity on addition of Zn^{2+} under the same conditions; the intensity of **1**+Mg^{2+} compared to **1**+Zn^{2+} was about 9 times greater. Upon an increase in the volume fraction of water in the mixed solvent system, the intensity of **1**+Zn^{2+} increases gradually, whilst the intensity of **1**+Mg^{2+} reduced dramatically. The intensity of **1**+Mg^{2+} was almost the same compared to free **1** when the water volume fraction was greater than 40%. By contrast, the intensity of **1**+Zn^{2+} was strong and stable; the intensity of **1**+Zn^{2+} compared to **1**+Mg^{2+} was about 22 times greater. On controlling the ratio of the DMF/H_2O mixed solvent system, **1** could identify Mg^{2+} in a DMF/H_2O (49/1, v/v) solvent system, and could also identify Zn^{2+} in a DMF/H_2O (1/4, v/v) solvent system. Similarly, the data for the absorption spectra are shown in Fig. 3B. Clearly, by controlling the different media conditions, **1** can selectively respond to either Mg^{2+} or Zn^{2+} ions.
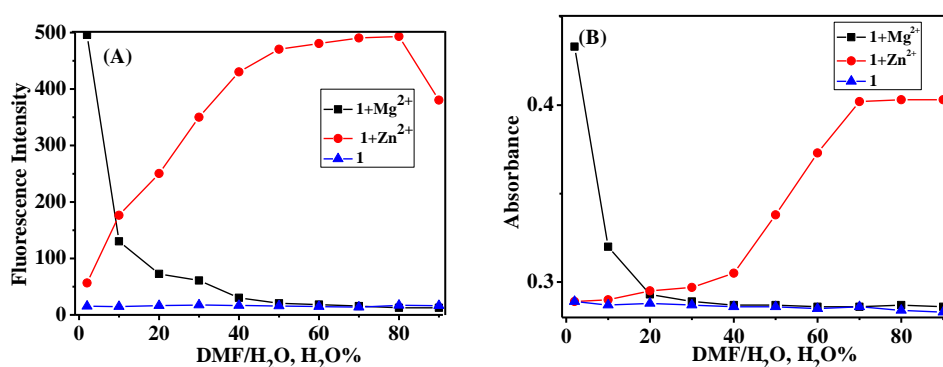
Fig. 3 The fluorescence intensity (A) and absorbance (B) of **1** (10 μM) with 20 eq. of Zn^{2+}, Mg^{2+} in DMF/H_2O mixed solvent; $\lambda_{ex} = 350$ nm; Zn^{2+}: $\lambda_{em} = 430$ nm; Mg^{2+}: $\lambda_{em} = 457$ nm; $\lambda_{max} = 355$ nm

Moreover, in DMF solvent, **1** showed ratiometric behaviour towards F^- (Fig. 4A). Upon addition of varying amounts of F^- ion lead to a decrease in the absorption at 290 nm, whilst the absorption band at 347 nm increased and red shifted to 360 nm. In addition, the absorption band at 420 nm blue shifted to 390 nm, and a distinct isosbestic point at 348 nm was observed indicating a

chemical interaction between receptor **1** and F$^-$ (Fig. 4B). Both intensive bands were attributed to H-bonding involving the phenolic O-H.
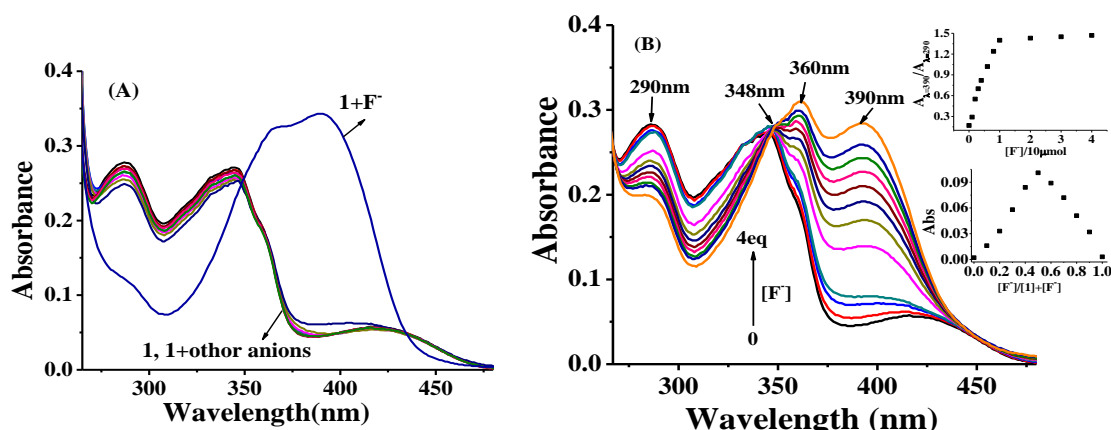
Fig. 4 (A) Absorption spectra of **1** (10 μM) upon the addition of 20 eq. of anions in DMF; (B)Absorbance spectra titration of **1** (10 μM) with F$^-$. Inset shows variation of ratio absorbance against the number of equivalents of ions and Job's plot data. A$_{390\ nm}$/A$_{290\ nm}$.

The stoichiometry of the complex of Zn^{2+}, Mg^{2+} and F$^-$ with **1** was determined by Job's plot and the molar ratio from the UV-vis absorption data (Figs. 1B, 2B and 4B inset). The plot revealed a 1:1 binding stoichiometry of **1** with ion. The association constants were estimated to be 6.9×10^4 (**1**-Zn^{2+}), 3.6×10^4 (**1**-Mg^{2+}) and 6.9×10^4 M^{-1} (**1**-F$^-$) by using a Benesi-Hildebrand plot assuming a 1:1 stoichiometry, respectively (Figs. S4~S6). The limits of detection (LOD = 3σ/slope) of **1** for Zn^{2+}, Mg^{-2+} and F$^-$ were 0.35, 0.21 and 0.36 μM, respectively (Figs. S7~S9).

In DMF/H$_2$O (1/4, v/v) solution, the absorbance ratio (A$_{355}$/A$_{420}$) of **1** (10 μM) for 20 eq. of Zn^{2+} and the effect of 20 eq. of coexisting ions on **1**-Zn^{2+} revealed that the other competing metal ions including Mg^{2+} did not interfere with the detection of Zn^{2+} (Fig. S10A). In DMF/H$_2$O (49/1, v/v) solution, the absorbance ratio (A$_{370}$/A$_{430}$) of **1** (10 μM) for 20 eq. of Mg^{2+} and the effect of 20 eq. of the coexisting ions on **1**-Mg^{2+} revealed that the other competing metal ions including Zn^{2+} did not interfere with the detection of Mg^{2+} (Fig. S10B). In DMF solution, the absorbance ratio (A$_{390}$/A$_{290}$) of **1** (10 μM) for 20 eq. of F$^-$ and the effect of 20 eq. of coexisting ions on **1**-F$^-$ revealed that the other competing anions did not interfere with the detection of F$^-$ (Fig. S10C). Hence, these results suggest that **1** could be a good ratiometric absorbance selective sensor for Zn^{2+}, Mg^{2+}, and F$^-$, in particular, conveniently distinguishing Zn^{2+} from Mg^{2+} and *visa visor*.

3.1.2 Fluorescence spectra characteristics for ions

To obtain insight into the fluorescent properties of **1** toward different ions in different medium, the emission changes were investigated with different ions. In DMF/H$_2$O (1/4, v/v) solution, when excited at 360 nm, **1** exhibited a weak fluorescence band (quantum yield, $\Phi_f = 0.02$) at 440 nm (Fig. 5A). Upon addition of the above metal ions, it can be seen that there is a great enhancement in the fluorescence intensity of Zn^{2+} ions with **1**, which could be clearly distinguished from the other metal ions. The fluorescent signal of **1** at 458 nm increases significantly ($\Phi_f = 0.37$) with a red shift to 458 nm observed, and prominent bright blue fluorescence was also observable under UV light (Fig. 5A, inset). The other metal ions including Mg^{2+} induce only slight changes in the fluorescence spectra. The weak fluorescence of **1** in the absence of Zn^{2+} can be attributed to rapid *cis-trans* isomerization across the C=N bond. The chelation of Zn^{2+} by **1** is not only responsible for chelation enhanced fluorescence (CHEF) but also seems to affect the intramolecular charge transfer (ICT) within the sensor [40, 41]. The electron-donating ability of the hydroxyl group at one end and electron-withdrawing ability of carbonyl group and imine at another end makes the sensor a potential ICT probe. However the ICT of **1** was affected due to chelation of **1** with Zn^{2+}, which ultimately resulted in a red shift of the emission spectrum of **1**. A Job's plot and the molar ratio of the fluorescence titrations revealed a 1:1 binding stoichiometry (Fig. 5B, inset); the association constant for Zn^{2+} was estimated to be 6.3×10^4 M^{-1} (Fig. S11), and the limit of detection was 53 nM (Fig. S12).
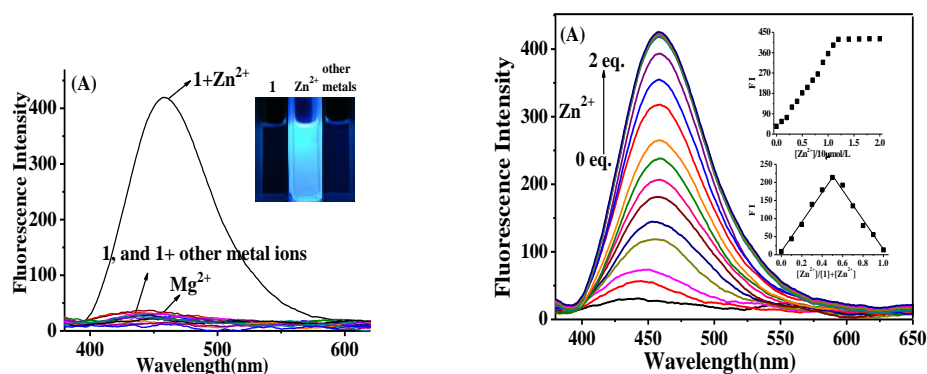
Fig. 5 (A) The fluorescence intensity of **1** (10 μM) with 20 eq. of metal ions in DMF/H$_2$O (1/4, v/v); Metal ions: Zn^{2+}, Mg^{2+}, Li$^+$, Na$^+$, K$^+$, Ca^{2+}, Hg^{2+}, Ba^{2+}, Pb^{2+}, Cd^{2+}, Co^{2+}, Ni^{2+}, Sr^{2+}, Cr^{3+}, Cu^{2+}, Ag$^+$, Al^{3+}, Fe^{3+}; (B) Fluorescence spectra titration of **1** (10 μM) with Zn^{2+}. Inset shows variation of fluorescence intensity against the number of equivalents of Zn^{2+} and Job's plot data. In DMF/H$_2$O (1/4, v/v), $\lambda_{ex} / \lambda_{em} = 360$ nm/458 nm.

In DMF/H$_2$O (49/1, v/v) solution, when excited at 350 nm, **1** also exhibited weak fluorescence

($\Phi_f = 0.02$); only the addition of Mg^{2+} led to a significant fluorescence enhancement ($\Phi_f = 0.39$) at 430 nm, while the other metal ions including Zn^{2+} induce only slight changes in the fluorescence spectra, suggesting **1** can act as an efficient Mg^{2+} selective fluorescence "turn-on" sensor based on the PET mechanism (Fig. 6A). The prominent blue fluorescence was also observable under UV light (Fig. 6A, inset). Coordination of Mg^{2+} to the oxygen atoms of the phenolic and nitrogen atoms of the imine moiety not only suppressed the photo-induced electron transfer (PET) from the imine nitrogen atoms to the coumarin moiety quenching process, but also increased the rigidity of the molecule by restricting free rotation of the single bond and thus resulting in a significant enhancement of the fluorescence intensity which is known as chelation enhanced fluorescence (CHEF) [42, 43]. A Job's plot and the molar ratio of the fluorescence titrations revealed a 1:1 binding stoichiometry (Fig. 6B, inset). The association constant for Mg^{2+} was estimated to be 2.7×10^4 M^{-1} (Fig. S13), and the limit of detection was determined to be 33 nM (Fig. S14).
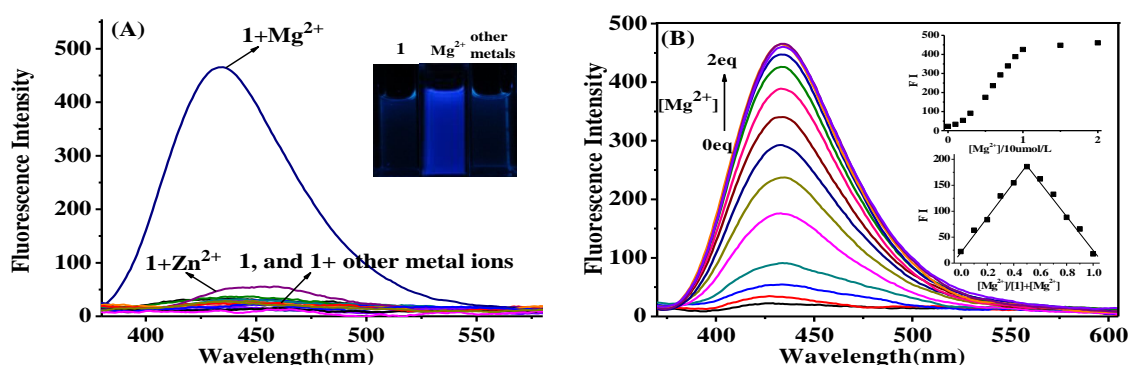
Fig. 6 (A) The fluorescence intensity of **1** (10 μM) with 20 eq. of metal ions in DMF/H_2O (98/2, v/v); (B) Fluorescence spectra for titration of **1** (10 μM) with Mg^{2+}. Inset shows variation of fluorescence intensity against the number of equivalents of Mg^{2+} and Job's plot data. in DMF/H_2O (49/1, v/v), λ_{ex} /λ_{em} = 350 nm/430 nm.

In DMF solvent, when the excitation was at 360 nm, in the absence or presence of anions (Cl^-, Br^-, I^-, NO_3^-, AcO^-, $H_2PO_4^-$, PF_6^-, ClO_4^-, HSO_4^-), it was shown that the fluorescence spectra of **1** did not undergo any significant change except when in the presence of F^- ion. Addition of the F^- ion results in enhanced fluorescence at 440 nm with a slightly bathochromic shift to 460 nm, exhibiting an "off-on" fluorescence emission (Fig. 7A), and the bright blue fluorescence could be observed under UV light (Fig. 7A, inset). Sensor **1** exhibits a higher affinity toward F^- ions because the hydroxyl groups of the two coumain units can participate in cooperative hydrogen bonding and then undergo further deprotonation. The emission intensities became constant when the amount of F^- added reached one equivalent (Fig. 7B). The Job's plot and the molar ratio of the fluorescence

titrations revealed a 1:1 binding stoichiometry (Fig. 7B, inset); the association constant for F$^-$ was estimated to be 7.7×10^4 M^{-1} (Fig. S15), and the limit of detection was found to be 17 nM (Fig. S16).
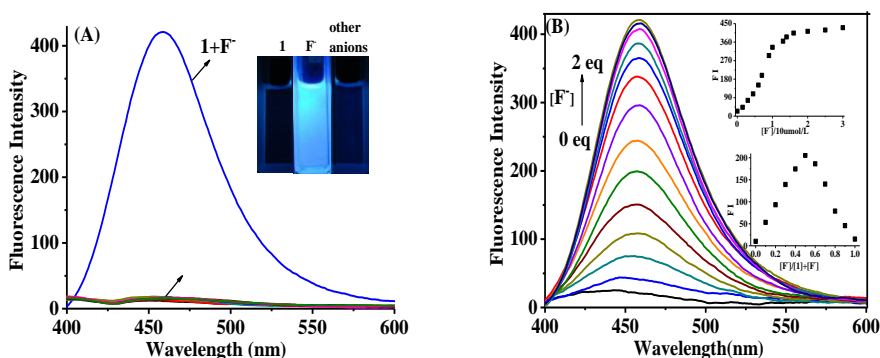
Fig. 7 (A) The fluorescence intensity of **1** (10 μM) with 20 eq. of anions in DMF; (B) Fluorescence spectra titration of **1** (10 μM) with F$^-$. Inset shows variation of fluorescence intensity against the number of equivalents of F$^-$ and Job's plot data in DMF, λ_{ex} /λ_{em} = 360 nm / 460 nm.

Many fluorescent sensors for Zn^{2+}/ Mg^{2+}/F$^-$ detection can only preform in solution, which limits their applications under special circumstances such as on-site detection *in situ*. To demonstrate the practical application, the filter paper of **1** was prepared. It was easily prepared by immersing a filter paper into the solution of **1** (1 mM) in DMF/H$_2$O (1/4, v/v) for Zn^{2+}, in DMF/H$_2$O (49/1, v/v) for Mg^{2+}, in DMF for F$^-$, and then exposing it to air to evaporate the solvent. After immersing in the Zn^{2+}/Mg^{2+}/F$^-$ solution for several seconds and drying in air, the fluorescence test strips showed an increase in fluorescence intensity with the Zn^{2+}/Mg^{2+}/F$^-$ concentration under the UV lamp (Fig. 8). The detection limits of the papers were as low as 1 μM of Zn^{2+}/F$^-$, 100 μM of Mg^{2+} ion.
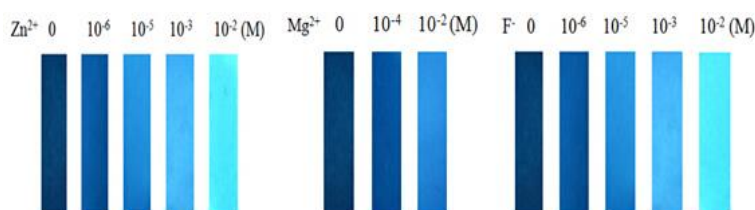
Fig. 8 Fluorescence changes of paper test strips for detecting Zn^{2+}, Mg^{2+}, F$^-$ ions in DMF/H$_2$O or DMF solution with different ion concentrations. The test papers were excited at 365 nm using a hand-held UV lamp.

To investigate the practical applicability of **1** as a multiple analyte selective fluorescent sensor, competition experiments of **1** (10 μM) treated with 20 eq. of the detection ion in the presence of other same concentration coexisting ions were carried out. In Fig. S17A, the other background

metal ions had little or no obvious interference with the detection of Zn^{2+} ions in DMF/H_2O (1/4, v/v), except for Co^{2+}, Cr^{3+}, Ni^{2+}, and Cu^{2+}. In Fig. S17B, the other background metal ions had little or no obvious interference with the detection of Mg^{2+} ions in DMF/H_2O (49/1, v/v), except for Hg^{2+}, Pb^{2+}, Cd^{2+}, Co^{2+} and Cu^{2+}. Hence, these results suggest that **1** could be a good fluorescence enhancement sensor for Zn^{2+} and Mg^{2+}. In particular, **1** can distinguish Zn^{2+} from Mg^{2+} or Mg^{2+} from Zn^{2+}, despite both having many common properties. In Fig. S17C, the other background anions had little or no obvious interference with the detection of F^- ions in DMF. Hence, these results suggest that **1** could be a fluorescence enhancement selective sensor for Zn^{2+}, Mg^{2+}, and F^-.

3.2 The complex characteristics of *1* with ions

3.2.1 Characteristics of isothermal titration calorimetry

Isothermal titration calorimetry can provide complete thermodynamic parameters of the binding enthalpy change (ΔH), entropy change (ΔS), binding constant (K), and stoichiometry (n) from a single titration, and offers a direct means of characterizing the thermodynamic properties of molecule and ion interactions. The binding of **1** with Mg^{2+} or F^- was investigated by ITC in DMF solution at 288.15 K. The **1**-ion titration is shown in Figs. S18A and 18C together with the integrated heats per mole of injectant (Figs. 18B, 18D). When the ion concentration increases, the bonding process is exothermic, and then tended to saturate; the thermodynamic parameters are listed in Table S1. This indicated that the complexation of **1** with Mg^{2+} or with F^- was driven by both enthalpy and entropy. The values of $\Delta G°$ (Mg^{2+}: ΔG= - (149.71 ± 1.08) kJ·M^{-1}, F^-: $\Delta G°$= - (33.93 ± 1.33) kJ·M^{-1}) are less than zero, which indicates that the binding processes are spontaneous. The stoichiometry for the sensor bound to the ion was about 1:1, and the binding constant (K) was up to 10^6 M^{-1} and 10^4 M^{-1}, respectively. The ITC experimental results are consistent with those of the fluorescence and UV/vis spectra.

3.2.2 Characteristics of the complex of *1* with ions

To confirm the stoichiometry between the **1** and the Zn^{2+}, Mg^{2+} ion, an API-ES mass examinations were conducted (Fig. S19). Mass peaks at m/z 469.17 (calculated value 469.48) and 428.64 (calculated value 428.41) corresponding to [**1**+Zn]$^+$ and [**1**+Mg]$^+$ were clearly observed, which provided evidence for the formation of a 1:1 complex, and the results are consistent with the spectral data *vide infra*.

The IR spectra of **1**, **1**-Zn^{2+} or **1**-Mg^{2+} were measured in DMF medium (Figs. S20A and Fig. S20B). Comparison with the IR spectra of **1** before and after the addition of Zn^{2+} or Mg^{2+}, reveals that some IR peak were shifted. Specifically, the C-N peak of **1** at 1112 cm^{-1}, N-Zn^{2+} at 623 cm^{-1}, N-Mg^{2+} at 627 cm^{-1}, C=N peak of **1** at 1622 cm^{-1} changed on adding either Zn^{2+} or Mg^{2+}, which indicated the participation of the imino and hydroxyl in the complexation of the sensor with the ion. In Fig. S20C, comparison with the IR spectra of **1** before and after adding F$^-$ in DMF, revealed that the C=N peak of **1** at 1622 cm^{-1}, C-N at 1 622 cm^{-1}, and -OH at 3427 cm^{-1} had all changed on adding the F$^-$ ion, which indicated the participation of the hydroxyl in the complexation of the sensor with the ion.

To explore the sensing mechanism of **1** with the ions, ^{1}H NMR titrations were conducted. Fig. 9 is the ^{1}H NMR titration of **1** with Zn^{2+} in DMF-d$_7$/D$_2$O (4/1, v/v). On complexation of **1** with Zn^{2+}, the proton peaks of the imine shifted to lower field due to the reduction of electron density upon coordination to the metal ion. All protons of the coumarin moieties were shifted upfield from $\Delta\delta$ 0.042 ppm to 0.083 ppm. The ^{1}H NMR data demonstrated that the phenolic hydroxyl oxygen atom of the coumarin and the nitrogen atoms of imine are the binding sites.
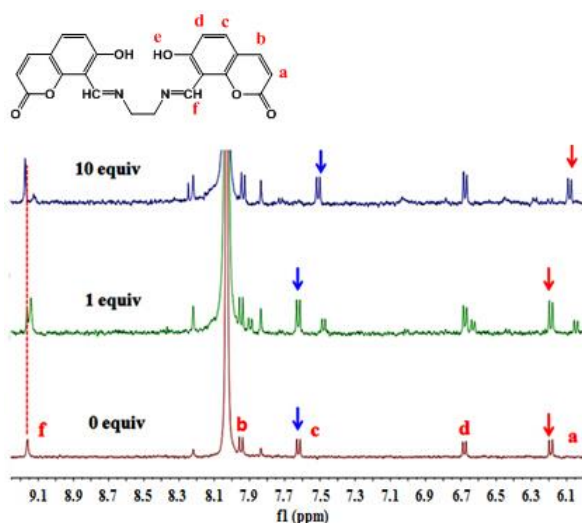
Fig. 9 ^{1}H NMR spectra in the absence and presence of Zn^{2+} for **1**.

The partial ^{1}H NMR spectra of **1** upon the addition of various amounts of Mg^{2+} in DMF are illustrated in the supporting information. On addition of 10 eq. of Mg^{2+} ion, no significant change was observed. After addition of 30 eq. of Mg^{2+}, the proton of hydroxyl group at 14.767 ppm disappeared. At the same time, the imine C-H peak at 9.16 ppm moved to 8.97 ppm, whilst the protons of the coumarin rings' all shifted to the upfield region ($\Delta\delta$ = 0.172 ppm ~ 0.567 ppm) as

shown in Fig. S21, which support the notion that the two nitrogens atoms of the imine, as well as two phenolic oxygens, can participate in binding with Mg^{2+}.

To examine the interaction between **1** and F^-, ^1H NMR titrations of **1** were investigated in the absence and the presence of F^- in DMSO-d_6 (Fig. 10). Upon addition of **1** eq. of F^-, the proton of hydroxyl group shifted downfield from 8.96 ppm to 10.16 ppm, whilst the proton of the imine revealed no change, but the protons of the coumarin moiety were shifted upfield ($\Delta\delta = 0.307$ ppm ~ 0.505 ppm). These results indicated the formation of hydrogen bonding between the fluoride and hydroxyl groups. On increasing the fluoride concentration to 5 eq., the proton of the hydroxyl group at 10.16 ppm disappeared and a new triplet at 16.06 ppm appeared, indicating the formation of a $[HF_2^-]$ species [44-46]. This deprotonation also caused the protons of the coumarin moiety to undergo upfield shifts of $\Delta\delta$ 0.059 ppm to 0.137 ppm, but the proton of imine shifted downfield by 0.342 ppm. The reorganization of the F^- included two steps: the first was the formation of a 1:1 stoichiometry complex through hydrogen bonding; the second was the deprotonation of the sensor with the formation of the HF_2^- anion. These results revealed the "off-on" optical switching mode of **1** with Zn^{2+}, Mg^{2+} and F^-, as shown in Scheme 2.
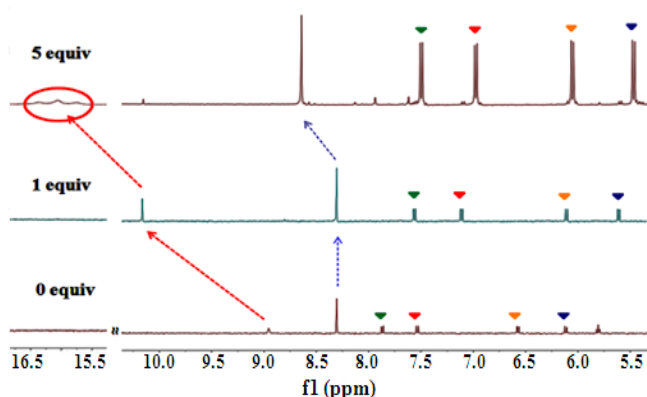
Fig. 10 ^1H NMR spectra in the absence and presence of F^- for **1**.
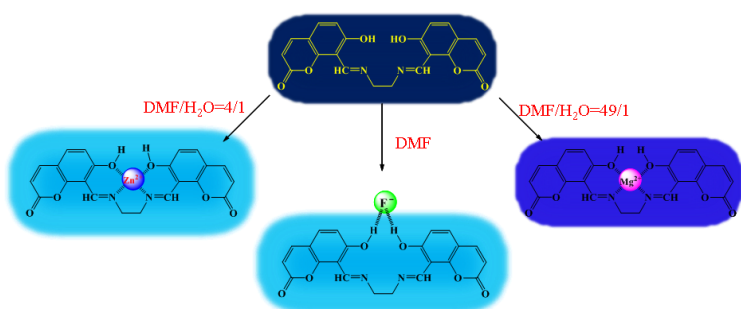
Scheme 2 Graphic of the proposed mechanism of the sensing of ions.

3.3 Fluorescence imaging of intercellular Zn^{2+}

The fluorescence imaging of **1** as a Zn^{2+} sensor in living cells was examined. Incubation of PC3 cells with 10 μM of **l** for 30 min at 37 °C gave almost no intracellular fluorescence as monitored by fluorescence microscopy. Figs. 11A and 11B show bright-field and fluorescence measurements. This was consistent with the incubation of the cells with 10 μM of **1**. When PC3 cells were incubated with growth medium containing 10 μM of **1** for 30 min, the same treatment with 50 μM of Zn^{2+} generated remarkable intracellular fluorescence (Fig. 11C). The fluorescence imaging measurements after treatment with **1** and Zn^{2+} confirmed that the cells were viable throughout the imaging experiments. The results suggested that **1** can penetrate the cell membrane in a short time and can be used to monitor intracellular Zn^{2+} in PC3 cells by *vitro* imaging and potentially *in vivo*.

Fig. 11 Fluorescence images of intracellular Zn^{2+} in PC3 cells. (A) Bright-field images of PC3 cells incubated with **1** (10 μM) at 37 °C for 30 min; (B) Fluorescence images of (A); (C) Fluorescence images of PC3 cells incubated with **1** and subsequent incubated with Zn^{2+} (50 μM) for 30 min.

4. Conclusion

With the aim of assaying metal ions and anions, a simple and multifunctional Schiff base fluorescence sensor **1** was synthesized. It is an excellent sensor exhibiting solvent-dependent, ion-tunable selectivity for Zn^{2+}, Mg^{2+} and F^- in different media. The outstanding selectivity of **1** allowed for the efficient detection and quantification of Zn^{2+} in DMF/H_2O (1/4, v/v) solution, Mg^{2+} in DMF/H_2O (49/1, v/v), F^- in DMF solution and these were not disrupted by common metal ions or anion ions. The presence of the o-hydroxy groups and the nature of the solvent play a crucial role in the selectivity for the metal ions and the switch of selectivity from Zn^{2+} to Mg^{2+} or F^-. The luminescence mechanism is as follows: the formation of a rigid framework between Schiff bases and Zn^{2+} inhibits the C=N isomerization, leading to fluorescence enhancement. Simultaneously, the chelation between the metal ion and the sensor causes a large CHEF combined with an ICT effect,

which induces the increase of fluorescence intensity and the wavelength red-shift. However, in DMF/H_2O (49/1, v/v) solution, various metal ions also have no interfere with the selectivity of **1** for Mg^{2+}, the recognition model is formation of a rigid framework between Schiff bases and Zn^{2+} which inhibits the PET procedure, leading to fluorescence enhancement. Furthermore, in DMF solution, **1** showed high selectivity for F^- by formation of multiple hydrogen-bonds and deprotonation resulting in fluorescence enhancement. Moreover, fluorescence microscopy confirmed that **1** can be used for monitoring Zn^{2+} in living PC3 cells with general fluorescence methods. These results provide a useful sensing strategy for the concept of a single chemosensor for multiple analytes. The present sensor is less expensive as it involves a facile step reaction with commercially available cheap chemicals. Also, derivatives of coumarin appear extremely useful for *in vivo* imaging applications and further exploration of these systems are currently underway in our laboratory.

Acknowledgments

References

[1] K. P. Carter, A. M. Young and A. E. Palmer, Fluorescent Sensors for Measuring Metal Ions in Living Systems, Chem. Rev., 114 (2014) 4564-4601.

[2] T. V. O' Halloran, Transition metals in control of gene expression, Science, 261 (1993) 715-725.

[3] N. Rujithamkul, L. Majlessi, C. Denoyelle, and G. Bordenave, Inhibition of IgG2a Production by Ig Allotype-Specific T Cells Can Be Mediated without T-B Cell Contact, Mol. Cell. Biochem., 188 (1998) 41-48.

[4] P. Jiang, Z. Guo, Fluorescent detection of zinc in biological systems: recent development on the design of chemosensors and biosensors, Chem. Rev., 248 (2004) 205-229.

[5] B. L. Vallee, K. H. Falchuk, The biochemical basis of zinc physiology, Physiol. Rev., 73 (1993) 79-118.

[6] H. Rubin, The logic of the Membrane, Magnesium, Mitosis (MMM) model for the regulation of animal cell proliferation, Arch. Biochem. Biophys., 458 (2007) 16-23.

[7] J. A. Cowan, Structural and catalytic chemistry of magnesium-dependent enzymes, Biometals, 15 (2002)

225-235.

[8] N. E. L Saris, E. Mervaala, H. Karppanen, J. A. Khawaja, A. Lewenstam, An update on physiological, clinical and analytical aspects Clin, Chem. Acta, 294 (2000) 1-26.

[9] J. Du, M. Hu, J. Fan and X. Peng, Fluorescent chemodosimeters using ''mild'' chemical events for the detection of small anions and cations in biological and environmental media, Chem. Soc. Rev., 41 (2012) 4511-4535.

[10] A. P. de Silva, H. Q. N. Gunaratne, T. Gunnlaugsson, A. J. M. Huxley, C. P. Mcoy, J. T. Rademacher and T. E. Rice, Signaling Recognition Events with Fluorescent Sensors and Switches, Chem. Rev., 97 (1997) 1515-1566.

[11] K. K-W. Lo, A. W.-T. Choi and W. H.-T. Law, Applications of luminescent inorganic and organometallic transition metal complexes as biomolecular and cellular probes, Dalton Trans., 41 (2012) 6021-6047.

[12] C. S. Bonnet and E. Tóth, MRI probes for sensing biologically relevant metal ions, Future Med. Chem., 2 (2010) 367-384.

[13] H. Zhu, J. Fan, B. Wang and X. Peng, Fluorescent, MRI, and colorimetric chemical sensors for the first-row d-block metal ions, Chem. Soc. Rev., 44 (2015) 4337-4366.

[14] L. E. Santos-Figueroa, M. E. Moragues, E. Climent, A. Agostini, R. Martínez-Máñez and F. Sancenón, Chromogenic and fluorogenic chemosensors and reagents for anions, A comprehensive review of the years 2010-2011, Chem. Soc. Rev., 42 (2013) 3489-3613.

[15] H. Chen, W. Gao, M. Zhu, H. Gao, J. Xue and Y. Li, A highly selective OFF-ON fluorescent sensor for zinc in aqueous solution and living cells, Chem. Commun., 46 (2010) 8389-8391

[16] M. Chen, X. Lv, Y. Liu, Y. Zhao, J. Liu, P. Wang and W. Guo, An 2-(2'-aminophenyl)benzoxazole-based OFF-ON fluorescent chemosensor for Zn^{2+} in aqueous solution, Org. Biomol. Chem., 9 (2011) 2345-2349.

[17] C. Zhang, Z. Liu, Y. Li, W. He, X. Gaod and Z. Guo, In vitro and in vivo imaging application of a 1,8-naphthalimide-derived Zn^{2+} fluorescent sensor with nuclear envelope penetrability. Chem. Commun., 49 (2013) 11430-11432.

[18] Z. Dong, X. Le, P. Zhou, C. Dong and J. Ma. An ''off-on-off'' fluorescent probe for the sequential detection of Zn^{2+} and hydrogen sulfide in aqueous solution, New J. Chem., 38 (2014) 1802-1808.

[19] O. B. Stepura and A. I. Martynow, Magnesium orotate in severe congestive heart failure (MACH), Int. J. Cardiol., 134 (2009) 145-147.

[20] S. Devaraj, Y.-K. Tsui, C.-Y. Chiang, Y.-P. Yen, A new dual functional sensor: Highly selective colorimetric chemosensor for Fe^{3+} and fluorescent sensor for Mg^{2+}. Spectrochimica Acta Part A: Molecular and Biomolecular Spectroscopy, 96 (2012) 594-599

[21] Y. Dong, J. Li, X. Jiang, F. Song, Y. Cheng, and C. Zhu, Na^+ Triggered Fluorescence Sensors for Mg^{2+} Detection Based on a Coumarin Salen Moiety, Org. Lett., 13 (2011) 2252-2255.

[22] D. Ray and P. K. Bharadwaj, A Coumarin-Derived Fluorescence Probe Selective for Magnesium, Inorg. Chem., 47 (2008) 2252-2254

[23] Y. Dong, X. Mao, X. Jiang, J. Hou, Y. Cheng and C. Zhu, L-Proline promoted fluorescent sensor for Mg^{2+} detection in a multicomponent sensory system, Chem. Commun., 47 (2011) 9450-9452.

[24] R. J. Carton, Review of the 2006 united states national research council report: fluoride in drinking water, Fluoride, 39 (2006) 163-172.

[25] S. Ayoob and A. K. Gupta, Fluoride in Drinking Water: A Review on the Status and Stress Effects,Crit. Rev. Environ. Sci. Technol., 36 (2006) 433-487.

[26] J.-T. Yeh, P. Venkatesan and S.-P. Wu, A highly selective turn-on fluorescent sensor for fluoride and its application in imaging of living cells. New J. Chem., 38 (2014) 6198-6204.

[27] C. Kar, S. Samanta, S. Mukherjee, B. K. Datta, A. Ramesh and G. Das, A simple and efficient fluorophoric probe for dual sensing of Fe^{3+} and F^-: application to bioimaging in native cellular iron pools and live cells, New J. Chem., 38 (2014) 2660-2669.

[28] S. Sharma, M. Singh Hundal and G. Hundal, Dual channel chromo/fluorogenic chemosensors for cyanide and fluoride ions-an example of in situ acid catalysis of the Strecker reaction for cyanide ion chemodosimetry, Org. Biomol. Chem., 11 (2013) 654-661.

[29] E. J. Song, H. Kim, I. H. Hwang, K. B. Kim, A. R. Kim, I. Noh and C. Kim, A single fluorescent chemosensor for multiple target ions: Recognitionof Zn^{2+} in 100% aqueous solution and F^- in organic solvent, Sensor and Actuators B, 195 (2014) 36-43.

[30] E. J. Song, J. Kang, G. R. You, G. J. Park, Y. Kim, S.-J. Kim, C. Kim and R. G. Harrison, A single molecule that acts as a fluorescence sensor for zinc and cadmium and a colorimetric sensor for cobalt, Dalton Trans., 42 (2013) 15514-15520.

[31] Y. W. Choi, G. J. Park, Y. J. Na, H. Y. Jo, S. A. Lee, G. R. You and C. Kim, A single Schiff base molecule for recognizing multiple metal ions: A fluorescence sensor for Zn(II) and Al(III) and colorimetric sensor for Fe(II) and Fe(III), Sensors and Actuators B, 194 (2014) 343-352.

[32] J. J. Lee, G. J. Park, Y. W. Choi, G. R. You, Y. S. Kim, S. Y. Lee and C. Kim, Detection of multiple analytes (CN^- and F^-) based on a simple pyrazine-derived chemosensor in aqueous solution: Experimental and theoretical approaches, Sensors and Actuators B, 207 (2015) 123-132

[33] M. Wang, F. Yan, Y. Zou, L. Chen, N. Yang and X. Zhou, Recognition of Cu^{2+} and Hg^{2+} in physiological

conditions by a new rhodamine based dual channel fluorescent probe, Sensors and Actuators B, 192 (2014) 512-521

[34] Y.-H. Zhao, X. Zeng, L. Mu, J. Li, C. Redshaw and G. Wei, A Reversible and Visible Colorimetric/Fluorescent Chemosensor for Al^{3+} and F^- ions with a Large Stoke's Shift, Sensors and Actuators B, 204 (2014) 450-458

[35] O. García-Beltrán, N. Mena, L. C. Friedrich, J. C. Netto-Ferreira, V. Vargas, F. H. Quina, M. T. Núñez and B. K. Cassels, Design and synthesis of a new coumarin-based 'turn-on' fluorescent probe selective for Cu^{2+}, Tetrahedron Letters, 53 (2012) 5280-5283.

[36] C. C. Woodroofe and S. J. Lippard, A Novel Two-Fluorophore Approach to Ratiometric Sensing of Zn^{2+}, J. Am. Chem. Soc., 125 (2003) 11458-11459

[37] T. Li, R. Fang, B. Wang, Y. Shao, J. Liu, S. Zhang and Z. Yang, A simple coumarin as a turn-on fluorescence sensor for Al(III) ions, Dalton Trans., 43 (2014) 2741-2743

[38] S. Zhu, W. Lin and L. Yuan, Development of a ratiometric fluorescent pH probe for cell imaging based on a coumarine quinoline platform, Dyes and Pigments 99 (2013) 465-471

[39] K. G. Reddie, W. H. Humphries, C. P. Bain, C. K. Payne, M. L. Kemp, and N. Murthy, Fluorescent Coumarin Thiols Measure Biological Redox Couples, Org. Lett., 14 (2012) 680-683

[40] S.-B. Liu, C.-F. Bi, Y.-H. Fan, Yu Zhao, P.-F. Zhang, Q.-D. Luo and D.-M. Zhang, Synthesis, characterization and crystal structure of a new fluorescent probe based on Schiff Base for the detection of Zinc (II), Inorganic Chemistry Communications, 14 (2011) 1297-1301.

[41] J.-S. Wu, W.-M. Liu, X.-Q. Zhuang, F. Wang, P.-F. Wang, S.-L. Tao, X.-H. Zhang, S.-K. Wu and S.-T. Lee, Fluorescence Turn On of Coumarin Derivatives by Metal Cations: A New Signaling Mechanism Based on C=N Isomerization, Org. Lett., 9 (2007) 33-36.

[42] R. Borthakur, U. Thapa, M. Asthana, S. Mitra, K. Ismail and R.A. Lal, A new dihydrazone based "turn on" fluorescent sensor for Zn(II) ion in aqueous medium, Journal of Photochemistry and Photobiology A, 301 (2015) 6-13.

[43] J. Wu, R. Sheng, W. Liu, P. Wang, H. Zhang and J. Ma, Tetrahedron. 68 (2012) 5458-5463.

[44] V. B. Bregovic, N. Basaric and K. Mlinaric-Majerski. Anion binding with urea and thiourea derivatives. Coordination Chemistry Reviews. 295 (2015) 80-124.

[45] D. Sharma, S. K. Sahoo, S. Chaudhary, R. K. Bera and J. F. Callan, Fluorescence 'turn-on' sensor for F^- derived from vitamin B_6 cofactor, Analyst, 138 (2013), 3646-3650.

[46] Q. Li, Y. Guo, J. Xu and S. Shao. Novel indole based colorimetric and ''turn on'' fluorescent sensors for

biologically important fluoride anion sensing, Journal of Photochemistry and Photobiology B, 103 (2011) 140-144.